Physics-Based Analytical Modeling of Electromigration Reliability for Multi-Segment Interconnect Wires

Jiangtao Peng, Hai-Bao Chen, Taeyoung Kim, Hengyang Zhao, Sheldon X.-D. Tan

***Abstract*—Electromigration (EM) is the major concern for the VLSI back end of the line (BEOL) reliabiliity. For EM modeling and assessment, one important problem is to perform fast EM time to failure analysis for practical interconnect layouts such as clock and power/ground networks consisting of many multi-segment wires. However, existing EM modeling and analysis techniques are mainly developed for a single wire. Although there are some early effects to resolve this issue, but there is no general analytic and compact model developed to estimate the EM-induced stress evolution, which is required to predict the time to failure. In this paper, we propose a new analytic expression hydrstatic stress calculation for general multi-segment interconnect wire with mutiple terminals. The new method is based on the Laplace transformation method on the Korhonen's equation with blocked atom flux boundary conditons. The analytical solutions in terms of a set of auxiliary basis functions using the complementary error function agree well with the numerical analysis results. Our analysis further demonstrates that using the first two dominant basis functions can lead to xx% error, which is sufficient for practical EM analysis.**

I. Introduction

Electromigration is considered the top killer for today's copper dual damascene interconnect technology. Recently there is a re-new interests in EM modeling and mitigation techniques as EM induced reliability is geting worse as technology advance. ITRS predicts that the EM induced life time of the interconnects will be reduced by half by each generation [1]. To make this situaiton more worse, many widely used EM models such as Black-Blech models are thought to be too conservative, which can lead to significant over designs [2].

Existing EM model and analysis techniques mainly focus on the simple straight line interconnect with two line end terminals. For practical VLSI chips, the interconnects such as clock and power grid networks typically consist of multi-branch metal segments representing a continuously connected, highly conductive metal (Cu) lines within one layer of metallization, terminating at diffusion barriers. The EM effects in those branches are not independent and they have to be considered simultaneously.

Recently some physics-based EM analysis methods for the TSV and power grid networks have been proposed based on solving the basic mass transport equations [3]–[6]. Those models treat the resistance changes of a wire over time as the atomic concentration changes due to atomic flux. Since these proposed methods solve the basic mass transport equations using the finite element method, they can only solve for very small structures such as one TSV structure. Complicated look-up table or models have to be built for different TSVs and wire segments for full-chip power grid analysis at reduced accuracy. To mitigate this problem, a more compact physics-based EM model was proposed recently in [7]. It is based on the hydrostatic stress diffusion equation [8]. However, this EM model still works for one single wire segment. Although the new EM model has been extended to deal with multiple branch tree wire based on projected steady-state stress. It still can't provide the time-dependent hydrostatic evolution of hydrostatic stress, which ultimately determines the failures for multi-branch interconnect wires.

Recently EM models for multi-branch interconnect tree have been proposed [9], [10]. In this approach, analytic solutions for stress development over time were dervied for three specific interconenct strucutres: the straight-line 3-terminal wires (figure I), the T-shape 4-terminal wires and the cross-shape 5-terminal wires. Those those analytic expressions are still can be applied to more general structures such as the multi-segment interconnect wires as showed Fig. **??**, which are commonly seen in the power/ground network in practical VLSI layouts.

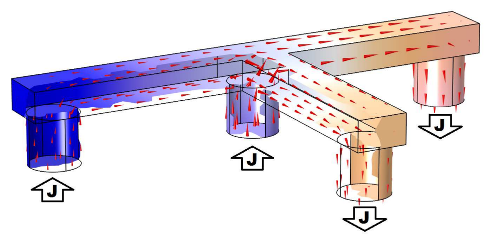

Fig. 1. Electrical current in a 3-terminal wire structure (J: current direction)

In this paper, we propose a new analytic expression hydrostatic stress calculation for general multi-segment interconnect wire with multiple terminals. The new method is based on the Laplace transformation method on the Korhonen's equation with blocked atom flux boundary conditions. The analytical solutions in terms of a set of auxiliary basis functions using the complementary error function agree well with the numerical analysis results. Our analysis further demonstrates that using the first two dominant basis functions can lead to xx% error, which is sufficient for practical EM analysis.

The remainder of the paper is organized as follows. In Section II, we induce the physics-based EM models and analysis methods for the stress evolution during EM in simple interconnect wires. Then we extend this analytic model to deal with a general multi-segment interconnect wire case in Section III. Experiment results and discussions for the stress evolution of EM effects for four-, five-, six-terminal interconnect wires are presented in Section IV. Concluding remarks are drawn in Section V.

II. Review of physics-based EM reliability modelling and analysis methods

EM has became of engineering interest since it was first observed as one of the primary failure mechanisms in aluminum IC conductors. Many researchers have studied the evolution of stress due to electromigration. Kirchheim proposed a physically based model in which generation of stress in grain boundaries during EM is caused by the annihilation and generation of vacancies. A physically based analytical model for mechanical stress evolution during EM was proposed by Korhonen [8] and further developed by many researchers [11], [12]. For a confined metal line, the hydrostatic stress distribution $\sigma(x,t)$ along the metal wire can be described by a one-dimensional diffusion-like equation, given by:

$$\frac{\partial\sigma(x,t)}{\partial t}=\frac{\partial}{\partial x}\left[\frac{D_aB\Omega}{kT}\left(\frac{\partial\sigma(x,t)}{\partial x}+\frac{Z^*e\rho}{\Omega}j\right)\right] \quad (1)$$

where σ is the hydrostatic stress, t is the time, D_a is the atomic diffusivity, B is the effective bulk modulus, Ω is the atomic volume, k is the Boltzman's constant, T is the absolute temperature, Z^* is the effective charge number, e is the electron charge, ρ is the resistivity, and j is the current density. The advantage of this model is that the evolution of hydrostatic stress in a confined line can be calculated in a closed-form expression, which has been widely used in EM analysis.

It should be noted that the closed-form expression reported in [8] is only applicable to a single wire case while it can not be used to calculate the hydrostatic stress during EM for multi-segment interconnect wires. In this paper, we extend the Korhonen equation (1) to allow for a general multi-segment interconnect wire. For the convenience of following description, we rewrite the Korhonen equation (1) as a compact form:

$$\frac{\partial\sigma(x,t)}{\partial t}=\frac{\partial}{\partial x}\left[\kappa\left(\frac{\partial\sigma(x,t)}{\partial x}+G\right)\right] \quad (2)$$

where $\kappa=\frac{D_aB\Omega}{kT}$ is the stress diffusivity affected by temperature T and $G=\frac{Z^*e\rho}{\Omega}j$ is the EM driving force. Moreover, $D_a=D_0e^{-\frac{E_a}{kT}}$ is the effective atomic diffusion coefficient. D_0 and E_a stand for the pre-exponential factor and the activation energy, respectively. The Korhonen equation (2) has differen analytical solutions with different boundary conditions (BCs). Following the idea in [8], we assume that the stress diffusivity κ does not depend on time. During the void nucleation phase of EM, the atom fluxes are blocked at both wire ends $x=0$ and $x=L$ at any moment in time. The initial stress value during the void nucleation phase is set to be zero. Thus, the closed-form solution of the stress evolution equation for a single segment wire can be given as follows [8]:

$$\begin{aligned}\sigma(x,t)=GL\{&\frac{1}{2}-\frac{x}{L}\\&-4\sum_{n=0}^{\infty}\frac{\cos((2n+1)\pi\frac{x}{L})}{(2n+1)^2\pi^2\exp((2n+1)^2\pi^2\frac{\kappa t}{L^2})}\}.\end{aligned} \quad (3)$$

By employing the analytical expression (3), the void nucleation time can be easily predicted. Assuming of course that the stress $\sigma(x,t)$ in the wire has reached a critical state stress value σ_{crit}, then the void nucleation time t_{nuc} can be obtained by solving the equation $\sigma(x,t_{nuc})=\sigma_{crit}$.

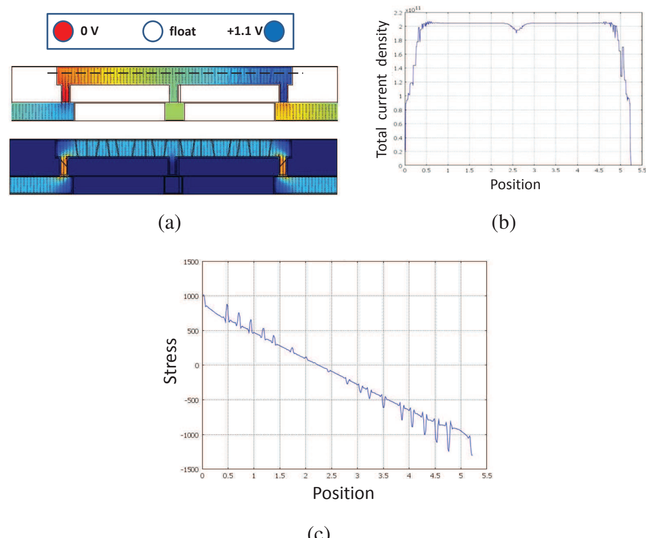

Fig. 2. (a) Three-terminal interconnect wire; (b) current density distributions; (c) hydrostatic stress distributions.

However, the existing analytical model (3) focuses only on a single segment wire. The research on EM-based stress evolutions of both void nucleation and growth phases for multi-segment interconnect wires is still a large and challenging problem. Due to the strong coupling between neighboring segments, EM reliability of multi-segment wires has become a recent major research for being a limiting factor in high performance circuit design. To further illustrate this, we consider a three-terminal interconnect wire loaded with DC currents as shown in Fig. 2(a). The finite element analysis tool COMSOL [**?**] can be used to calculate the hydrostatic stress along the interconnect wire. The distributions of the current density and the hydrostatic stress along this wire are shown in Fig. 2(b) and Fig. 2(c), respectively. Recent work [**?**] has report an analytical solution of EM-based stress evolution equation during the void nucleation phase. But it did not give an analytic form to model a general multi-segment interconnect wire. In this paper, for the first time, we will propose an analytic method to calculate the stress evolution considering EM effects during the void nucleation phase for multi-segment interconnect wires.

III. Accurate analytical modeling for hydrostatic stress evolution

In this paper, an accurate analytical modeling for transient hydrostatic stress analysis for a general realistic interconnect structure as shown in Fig.3, which represents a long metal wire with a number of the voltage and current ports. Since many complex interconnect structures such as power grids could be decomposed to hierarchically in smaller interconnect components, the accurate analytic closed-form expressions describing hydrostatic stress evolution for multi-branch interconnect trees will lay the groundwork for the EM reliability analysis of complex interconnect networks. Based on the Laplace transformation technique, an accurate closed-form expression during the void nucleation phase for the long metal wire shown in Fig.3 will be proposed.

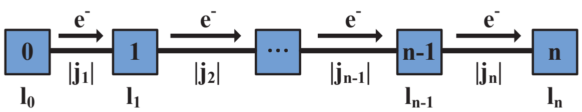

Fig. 3. An example of general realistic interconnect structure.

The stress evolution process for each segment in Fig.3 is described by the Korhonen equation. Stress evolution equations for each segment are coupled to each other by the boundary conditions representing the continuity of stress and fluxes at the junctions in the long metal wire. The general system of equation in this case can be described as follows:

$$
\begin{aligned}
&\frac{\partial \sigma_1}{\partial t} = \frac{\partial}{\partial x}[\kappa_1(\frac{\partial \sigma_1}{\partial x} + G_1)],\ l_0 \leq x \leq l_1\\
&\frac{\partial \sigma_2}{\partial t} = \frac{\partial}{\partial x}[\kappa_2(\frac{\partial \sigma_2}{\partial x} + G_2)],\ l_1 \leq x \leq l_2,\\
&\cdots\cdots\\
&\frac{\partial \sigma_{n-1}}{\partial t} = \frac{\partial}{\partial x}[\kappa_{n-1}(\frac{\partial \sigma_{n-1}}{\partial x} + G_{n-1})],\ l_{n-2} \leq x \leq l_{n-1},\\
&\frac{\partial \sigma_n}{\partial t} = \frac{\partial}{\partial x}[\kappa_n(\frac{\partial \sigma_n}{\partial x} + G_n)],\ l_{n-1} \leq x \leq l_n.
\end{aligned} \tag{4}
$$

In (4), κ_i and G_i $(i = 1, 2, \cdots, n)$ are the stress diffusivity and the EM driving force for each segment wire. Boundary conditions for these equations are given as the follows:

$$
\begin{aligned}
&\kappa_1(\frac{\partial \sigma_1}{\partial x} + G_1) = 0,\ x = l_0,\\
&\sigma_1 = \sigma_2,\ x = l_1,\\
&\kappa_1(\frac{\partial \sigma_1}{\partial x} + G_1) = \kappa_2(\frac{\partial \sigma_2}{\partial x} + G_2),\ x = l_1,\\
&\sigma_2 = \sigma_3,\ x = l_2,\\
&\kappa_2(\frac{\partial \sigma_2}{\partial x} + G_2) = \kappa_3(\frac{\partial \sigma_3}{\partial x} + G_3),\ x = l_2,\\
&\cdots\cdots\\
&\kappa_n(\frac{\partial \sigma_n}{\partial x} + G_n) = 0,\ x = l_n.
\end{aligned} \tag{5}
$$

Initial conditions for the void nucleation phase are given by $\sigma_i = 0$ at $t = 0$ at each segment. The Laplace transformation technique can be used to obtain an accurate closed-form expression for the void stress evolution equations (4). For the sake of simplicity, we need to assume that $\kappa_1 = \kappa_2 = \cdots = \kappa_k$. After transforming (4)-(5) by the Laplace transformation technique, we get a system of ordinary differential equations (ODEs). In order to derive the solution of each ODE, we first need to introduce the following notations:

$$
\begin{aligned}
&\xi^i_{n,1} = l_n + 2m(l_n - l_0) - x,\\
&\xi^i_{n,2} = (2l_n - l_0) + 2m(l_n - l_0) - x,\\
&\xi^i_{n,2j+1} = (2l_n - l_j) + 2m(l_n - l_0) - x,\\
&\xi^i_{n,2j+2} = \begin{cases} (2l_n - 2l_0 + l_j) + 2m(l_n - l_0) - x, \\ \qquad\qquad 0 < j < i, \\ l_j + 2m(l_n - l_0) - x,\ i \leq j \leq n-1, \end{cases}\\
&\eta^i_{n,1} = (l_n - 2l_0) + 2m(l_n - l_0) + x,\\
&\eta^i_{n,2} = -l_0 + 2m(l_n - l_0) + x,\\
&\eta^i_{n,2j+1} = (l_j - 2l_0) + 2m(l_n - l_0) + x,\\
&\eta^i_{n,2j+2} = \begin{cases} -l_j + 2m(l_n - l_0) + x,\ 0 < j < i, \\ (2l_n - l_j - 2l_0) + 2m(l_n - l_0) + x, \\ \qquad\qquad i \leq j \leq n-1. \end{cases}
\end{aligned} \tag{6}
$$

Similar to the analytical method introduced in [?], we need to construct the following basic function:

$$
g(x,t) = 2\sqrt{\frac{\kappa t}{\pi}}e^{-\frac{x^2}{4\kappa t}} - x \times \mathtt{erfc}\{\frac{x}{2\sqrt{\kappa t}}\}. \tag{7}
$$

where the complementary error function $\mathtt{erfc}\{x\}$ is defined as $\mathtt{erfc}\{x\} = \frac{2}{\sqrt{\pi}}\int_x^{+\infty} e^{-t^2}dt$. Thus, a general form of analytical solutions of stress evolution equations for all segments can be written as follows

$$
\begin{aligned}
\sigma_{n,i}(x,t) = &-\sum_{m=0}^{+\infty}\{G_n g(\xi^i_{n,1}, t) - G_1 g(\xi^i_{n,2}, t)\\
&- \sum_{j=1}^{n-1}\frac{G_{j+1} - G_j}{2}(g(\xi^i_{n,2j+1}, t) - g(\xi^i_{n,2j+2}, t))\}\\
&- \sum_{m=0}^{+\infty}\{G_n g(\eta^i_{n,1}, t) - G_1 g(\eta^i_{n,2}, t)\\
&- \sum_{j=1}^{n-1}\frac{G_{j+1} - G_j}{2}(g(\eta^i_{n,2j+1}, t) - g(\eta^i_{n,2j+2}, t))\}.
\end{aligned} \tag{8}
$$

It should be noted that the present analysis method in analytical characterization is similar to what has been reported in our early work of analytical modeling of electromigration for multi-branch interconnect tree. However, the purpose of this paper is not to develop any new analysis method, but to illustrate the closed-form expression for the solution of stress evolution equations for more complex interconnect trees embedded in the frequently employed circuits.

IV. Experimental results and discussions

In order to show the accuracy of the proposed model of EM reliability for multi-branch interconnect three with line structure shown in Fig. 3, the analytical solution (8) of stress evolution equations is calculated with the MATLAB enviroment, and we also compare the results from (8) with those obtained by the finite element tool COMSOL [?]. In our experiments, we test three cases of interconnect tree structure by changing n in (8) which is the number of wire segments in the interconnect tree. In the simulations to be described below, the following parameter values will be used: $Z^* = 10$, $\rho = 3 \times 10^{-8}\Omega/m$, $\Omega = 8.78 \times 10^{-30}m^3$, $B = 5.5 \times 10^{10}Pa$, $D_0 = 5.5 \times 10^{-5}m^2/s$, $E_a = 1.1eV$, $e = 1.6 \times 10^{-19}C$, $k = 1.38 \times 10^{-23}J/K$, and $T = 350K$.

A. Four-terminal interconnect wire ($n = 3$)

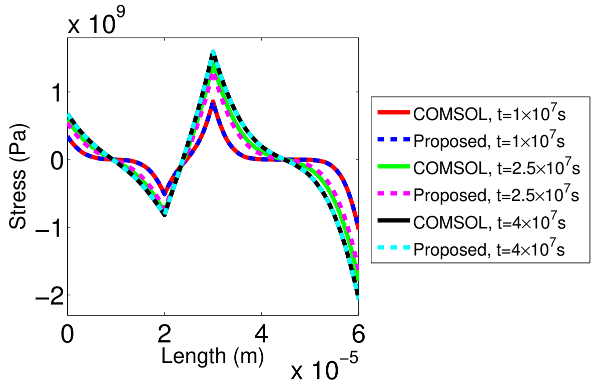

(a)

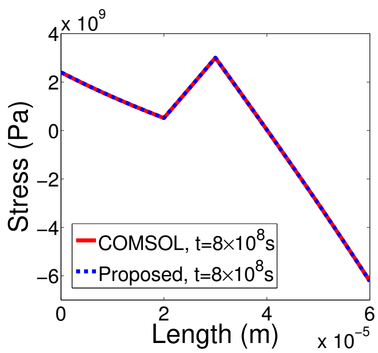

(b)

Fig. 4. The experiments results of straight line at changing temperatures, $j_1 = 2 \times 10^{10}A/m^2$, $j_2 = 6 \times 10^{10}A/m^2$ (a) the comparison of stress evolution at square wave temperature at a fixed time; (b) the comparison of stress evolution at sine wave temperature at a fixed time; (c) the comparison of stress evolution at square wave temperature at a fixed position; (d) the comparison of stress evolution at sine wave temperature at a fixed position

We first analyze the four-terminal interconnect tree with three wire segments with the current flow directions as shown in Fig. []. A constant current density of $j_1 =??$ is applied in the left segment, $j_2 =$ is used to stress the middle wire segment, and $j_3 =$ represent the current density of the right wire segment. The lengths for each wire segment in this interconnect tree are set to be $?m$, $?m$, and $?m$, respectively.

We first analyze the 3-terminal interconnect tree with two segments with the current flow directions as showed in Fig.**??**. Fig.**??** shows obtained evolution of the stress distribution. From Fig.**??** and Fig.**??**, analytical solution obtained with the proposed method fits well to the results of the numerical simulation at every time instance. For a fixed position shown in Fig.**??** and Fig.**??**, the stress changes in agreement with the

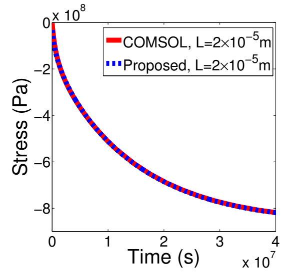

(a)

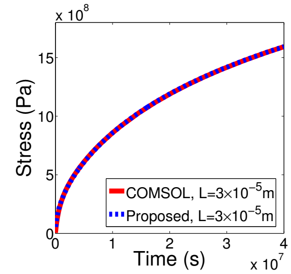

(b)

Fig. 5. The experiments results of straight line at changing temperatures, $j_1 = 2 \times 10^{10}A/m^2$, $j_2 = 6 \times 10^{10}A/m^2$ (a) the comparison of stress evolution at square wave temperature at a fixed time; (b) the comparison of stress evolution at sine wave temperature at a fixed time; (c) the comparison of stress evolution at square wave temperature at a fixed position; (d) the comparison of stress evolution at sine wave temperature at a fixed position

varying temperatures. In the case of square ware temperature, when temperature rises up to $380K$, the stress is going through dramatic changes. On the contrary, when temperature is $320K$, the stress is smoothly continuous. In the case of sine wave temperature, when temperature falls down to below $250K$, the stress has a process of slow change. And average temperature is useless for the interconnect tree analysis. Thermal effects depended on the varying temperature are remarkable.

We first apply the COMSOL to compute an accurate numerical solution of (1). We set the width of 3D interconnect tree as $10^{-8}m$, considering the thin and narrow interconnect line. Then we use the proposed approach to estimate the stress in MATLAB. Comparisons are shown in Fig. **??**, Fig. **??**, and Fig. **??**.

B. Five-terminal interconnect wire ($n = 4$)

C. Six-terminal interconnect wire ($n = 5$)

V. Conclusion

In this paper, we have proposed a new analysis method for multi-segment wires considering EM effects during the void nucleation phase. The new analytical model shows an excellent agreement with the detailed numerical analysis obtained from COMSOL.

References

[1] "International technology roadmap for semiconductors (ITRS), 2014 update," 2012. http://public.itrs.net.

[2] B. Bailey, "Thermally Challenged," in *Semiconductor Engineering*, 2013.

[3] J. S. Pak, M. Pathak, S. K. Lim, and D. Pan, "Modeling of electromigration in through-silicon-via based 3D IC," in *Electronic Components and Technology Conference (ECTC), 2011 IEEE 61st*, pp. 1420–1427, 2011.

[4] M. Pathak, J. S. Pak, D. Pan, and S. K. Lim, "Electromigration modeling and full-chip reliability analysis for BEOL interconnect in TSV-based 3D ICs," in *Computer-Aided Design (ICCAD), 2011 IEEE/ACM International Conference on*, pp. 555–562, 2011.

[5] X. Zhao, Y. Wan, M. Scheuermann, and S. K. Lim, "Transient modeling of TSV-wire electromigration and lifetime analysis of power distribution network for 3D ICs," in *Computer-Aided Design (ICCAD), 2013 IEEE/ACM International Conference on*, pp. 363–370, 2013.

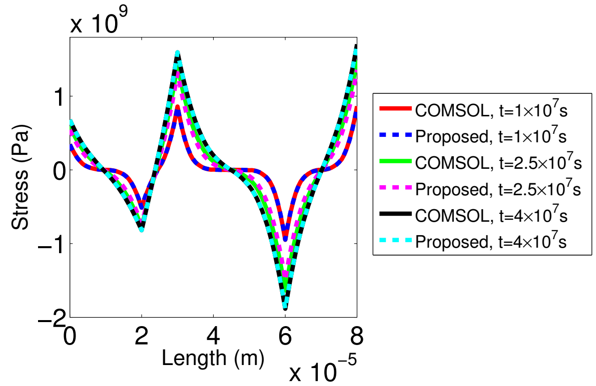

(a)

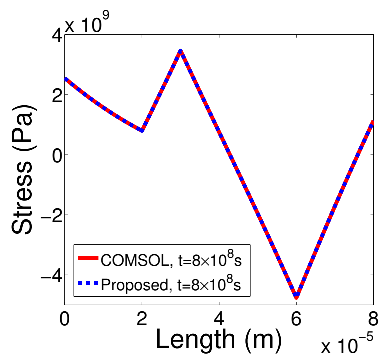

(b)

Fig. 6. The experiments results of straight line at changing temperatures, $j_1 = 2 \times 10^{10} A/m^2,\ j_2 = 6 \times 10^{10} A/m^2$ (a) the comparison of stress evolution at square wave temperature at a fixed time; (b) the comparison of stress evolution at sine wave temperature at a fixed time; (c) the comparison of stress evolution at square wave temperature at a fixed position; (d) the comparison of stress evolution at sine wave temperature at a fixed position

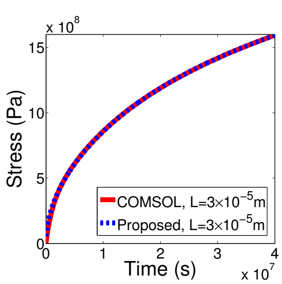

(a)

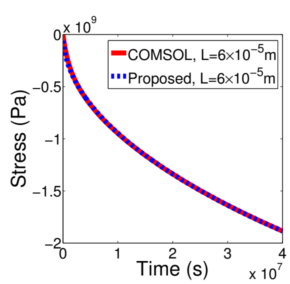

(b)

Fig. 7. The experiments results of straight line at changing temperatures, $j_1 = 2 \times 10^{10} A/m^2,\ j_2 = 6 \times 10^{10} A/m^2$ (a) the comparison of stress evolution at square wave temperature at a fixed time; (b) the comparison of stress evolution at sine wave temperature at a fixed time; (c) the comparison of stress evolution at square wave temperature at a fixed position; (d) the comparison of stress evolution at sine wave temperature at a fixed position

[6] J. Pak, S. K. Lim, and D. Z. Pan, "Electromigration study for multi-scale power/ground vias in TSV-based 3D ICs," in *Computer-Aided Design (ICCAD), 2013 IEEE/ACM International Conference on*, pp. 379–386, 2013.

[7] X. Huang, T. Yu, V. Sukharev, and S. X.-D. Tan, "Physics-based electromigration assessment for power grid networks," in *Proc. Design Automation Conf. (DAC)*, June 2014.

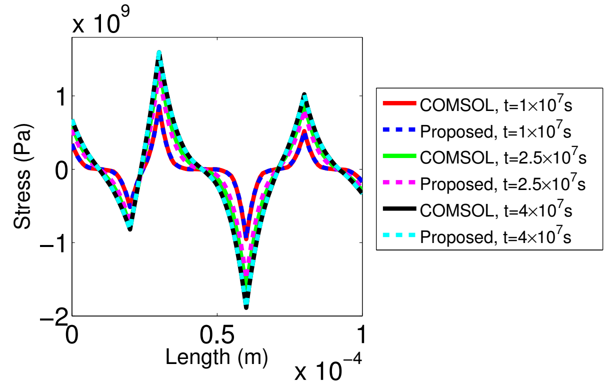

(a)

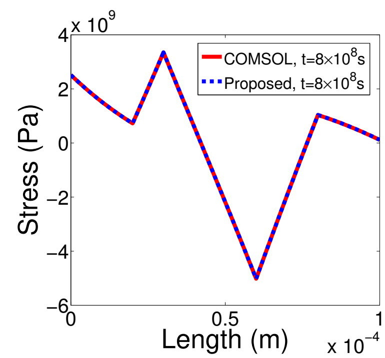

(b)

Fig. 8. the

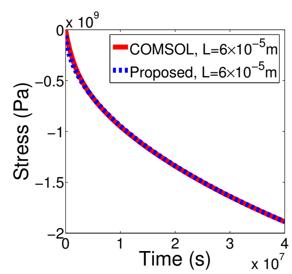

(a)

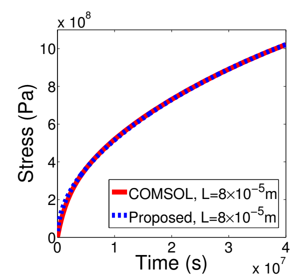

(b)

Fig. 9. The experiments results of straight line at changing temperatures, $j_1 = 2 \times 10^{10} A/m^2,\ j_2 = 6 \times 10^{10} A/m^2$ (a) the comparison of stress evolution at square wave temperature at a fixed time; (b) the comparison of stress evolution at sine wave temperature at a fixed time; (c) the comparison of stress evolution at square wave temperature at a fixed position; (d) the comparison of stress evolution at sine wave temperature at a fixed position

[8] M. A. Korhonen, P. Borgesen, K. N. Tu, and C. Y. Li, "Stress Evolution Due to Electromigration in Confined Metal Lines," *Journal of Applied Physics*, vol. 73, no. 8, pp. 3790–3799, 1993.

[9] H. Chen, S. X.-D. Tan, V. Sukharev, X. Huang, and T. Kim, "Interconnect reliability modeling and analysis for multi-branch interconnect trees," in *Proc. Design Automation Conf. (DAC)*, June 2015.

[10] H. Chen, X. Tan, X. Huang, T. Kim, and V. Sukharev, "Analytical modeling and characterization of electromigration effects for multi-branch interconnect trees," *IEEE Trans. on Computer-Aided Design of Integrated Circuits and Systems*, vol. 35, pp. 1811–1824, Nov. 2016.

[11] J. J. Clement, S. P. Riege, R. Cvijetic, and C. V. Thompson, "Methodology for Electromigration Critical Threshold Design Rule Evaluation,"

IEEE Trans. on Computer-Aided Design of Integrated Circuits and Systems, vol. 18, no. 5, pp. 576–581, 1999.
[12] V. Sukharev, X. Huang, and S. X.-D. Tan, "Electromigration Induced Stress Evolution Under Alternate Current and Pulse Current Loads," *Journal of Applied Physics*, vol. 118, pp. 034504–1–034504–10, 2015.